Influence of storm trajectory on the stable isotope composition of precipitation at Inuvik, NT

Loucas Diamant-Boustead & Christopher R. Burn
Carleton University, Ottawa, Ontario, Canada

ABSTRACT

Stable-isotope ratios in ice-wedge ice have been used to reconstruct winter conditions in Siberia and eastern Beringia. Such reconstructions assume that temperature is the principal influence on the isotopic composition of precipitation and, hence, wedge ice. Archived data for over 100 precipitation samples, collected between August 2015 and August 2018 at Inuvik, NT, indicate two distinct populations of $\delta^{18}O$ values for summer and winter. The regression equation for $\delta^{18}O$ (‰) on mean temperature (T, °C) for the day of precipitation is $\delta^{18}O = 0.3T - 19.3$ ($R^2 = 0.59$, $p < 0.01$). For summer, the equation is $\delta^{18}O = 0.19T - 18.2$ ($R^2 = 0.01$, $p = 0.007$), and for winter $\delta^{18}O = 0.16T - 22.2$ ($R^2 = 0.15$, $p = 0.02$). The difference between the seasons dominates the regression when all data are pooled, but seasonal data indicate low to no relation between the variables. NOAA's HYSPLIT model was used to trace storms back to where the synoptic system formed as well as the trajectory taken to reach Inuvik. Systems that travel over mountains to reach Inuvik experience considerable fractionation whereas systems from the proximal Beaufort Sea do not. The $\delta^{18}O$ values for systems originating from the north, south, and west were statistically indistinguishable in both seasons, but southerly systems arrived with the warmest conditions in winter. Separate bulk samples of monthly precipitation collected from 1985–1995 provided a stronger relation between $\delta^{18}O$ values and monthly mean temperature, but R^2 (0.28) was still low.

1 INTRODUCTION

Significant climate changes have occurred recently in the Arctic with greater warming than in other regions of the Earth (Chylek et al. 2022). Arctic amplification is partly a result of reduced terrestrial snow and ice cover, diminishing sea-ice coverage, and changes in atmospheric and oceanic circulation patterns (Serreze and Barry 2011). Considerable effort is underway to understand the extent of past changes in temperature as analogues for potential future climates. The stable isotope composition of ground ice can be used to reconstruct former climate conditions, especially through examination of ice-wedge ice. Wedge ice samples collected from Russia and the western Canadian Arctic have indicated warming during winter since the mid-Holocene (Opel et al. 2017; Holland et al. 2020).

The stable isotope composition in meteoric waters is defined by the ratios of ^{18}O:^{16}O and ^{2}H:^{1}H, relative to Vienna Standard Mean Ocean Water (VSMOW; Gonfiantini 1978) via δ notation, where for ^{18}O:

$$\delta^{18}O = \frac{\frac{^{18}O}{^{16}O}_{sample} - \frac{^{18}O}{^{16}O}_{VSMOW}}{\frac{^{18}O}{^{16}O}_{VSMOW}} \times 1000 \qquad [1]$$

and for hydrogen, δD, with D = ^{2}H. Characteristically, the concentration in ground ice is less than in VSMOW, due to depletion of heavy isotopes by fractionation during precipitation while the air mass is in transit from the source of vapour (Dansgaard 1964). Fractionation is the preferential incorporation of heavy isotopes into the lower energy phase (Dansgaard 1964). There is a strong linear relationship between $\delta^{18}O$ and δD in air masses. Craig (1961) presented the Global Meteoric Water Line (GMWL, eq. 2), representative of the general relation between these isotope compositions in precipitation.

$$\delta D = 8\,\delta^{18}O + 10 \qquad [2]$$

The GMWL is a result of proportionate fractionation of oxygen and hydrogen isotopes during phase change. As an airmass travels from its origin, it becomes depleted in these heavy isotopes, which are preferentially precipitated. The extent of depletion depends on the origin of the air mass, its trajectory, and the temperature during condensation (Dansgaard 1964).

Temperature (T) has been regarded as the most important variable associated with the isotopic composition of precipitation. Porter et al. (2016) and Kostrova et al. (2020) reported $\delta^{18}O$:T ratios of 0.41‰ $°C^{-1}$ from continental polar North America and 0.50‰ $°C^{-1}$ from Siberia. Dansgaard (1964) determined the initial relation between these variables for Greenland and North Atlantic stations as:

$$\delta^{18}O = 0.69T - 13.6 \qquad [3]$$

Equation 3 indicates that lower values of $\delta^{18}O$ are characteristically associated with cooler conditions.

Variations in isotopic concentrations have been used to distinguish massive and pore ice bodies in permafrost in stratigraphic terms and with respect to the climate when the ice formed (Mackay 1983a; Burn et al. 1986; Kotler and Burn 2000). Recently, the stable isotope composition of wedge ice has been presented as a winter climate proxy that is interpreted along the chronological sequence of veins in an ice wedge (Meyer et al. 2015; Opel et al. 2017).

https://doi.org/10.52381/ICOP2024.77.1

In this paper, the influences on the isotopic composition in precipitation of air-mass origin and trajectory are assessed for storms at Inuvik in the western Canadian Arctic. Samples of rain or snowfall were collected storm-by-storm at Inuvik for determination of $\delta^{18}O$ and δD in precipitation by Fritz et al. (2021). We used the NOAA HYSPLIT model to estimate the origin and back-trajectories of storm systems for which Inuvik temperature and precipitation isotope data are available between August 2015 and August 2018.

We also examined the $\delta^{18}O$:T relation for integrated samples of monthly precipitation collected between December 1985 and May 1995 at Inuvik Airport. The purpose was to determine whether $\delta^{18}O$:T relations derived on an event-by-event basis were replicated at a monthly time scale.

2 Study Area

Inuvik (68.36˚ N, 133.72˚ W; Figure 1) is located on the east side of the Mackenzie Delta, Northwest Territories. The town is in the broad plains east of the Western Cordillera, at an elevation of 15 m a.s.l. Air masses travelling from moisture sources to the south or west must cross these mountains, which reach over 4000 m a.s.l. close to the Pacific coast. The Beaufort Sea is about 100 km north of Inuvik. The land to the east is the flat and rolling terrain of the Interior Plains and Canadian Shield.

From 1991–2020, the mean annual temperature at Inuvik was -6.7 °C, an increase of 3.2 °C relative to the 1951–1980 mean (Schetselaar et al. 2023). The town has a monthly mean temperature below 0 °C between October and April. The coldest month is January, with a mean monthly temperature of -24.4 °C. In June through August, the mean temperature remains above 10 °C. Annual mean air temperatures have been rising within the region since 1971 (Thienpont et al. 2013). The rate of increase has been 0.77 °C/decade at Inuvik (Schetselaar et al. 2023).

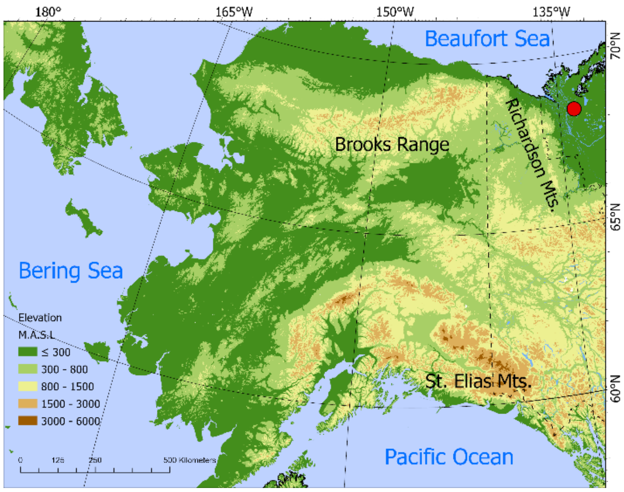

Figure 1. The western Canadian Arctic mainland and Alaska. Inuvik is indicated by the red circle in the northeastern corner of the map.

3 Methods

3.1 Precipitation 2015–2018

Fritz et al. (2021, 2022) collected 134 precipitation samples between August 2015 and August 2018 at the Aurora Research Institute in Inuvik. Samples were analyzed for δD and $\delta^{18}O$ at the Alfred Wegener Institute in Potsdam, Germany, and the results posted on the PANGEA database (Fritz et al. 2021). We combined these stable isotope values with amount of precipitation and the mean daily temperature on days with rain or snow at the Inuvik Airport (Environment Canada 2023).

3.2 HYSPLIT Model

The NOAA Hybrid Single-Particle Lagrangian Integrated Trajectory (HYSPLIT) model is a tool that simulates diffusion and movement within the atmosphere (Stein et al. 2015). The model was run for the dates of samples that could be confidently assigned to a specific precipitation event. Simulations were run using the READY web-interface. Single back-trajectories from Inuvik were generated with the 'normal' trajectory option. This allows for back-trajectories to be calculated for 315 hours (13 days), often leading to the source of the airmass, with the purpose of identifying the origin of precipitation. The National Weather Service's National Centers for Environmental Prediction Global Data Assimilation System (0.5˚ lat/long resolution) was the chosen meteorological grid model. Back-trajectories were calculated at three different levels in the atmosphere (250, 500, and 1000 m a.s.l). Commonly, these trajectories originated from the same location, but if they did not, the location with the majority was chosen.

3.3 Data Considerations

Of the 134 samples collected by Fritz et al. (2021), only 111 were used in the analysis. One sample was excluded by Fritz et al. (2022) due to an exceedingly low d-excess value of -17.8 ($\delta D - 8\delta^{18}O$); two samples were omitted due to labelling errors; nineteen were excluded due to inconclusive results from the HYSPLIT model (3), or an inability to confidently identify the storm responsible for the precipitation (16). One sample originated from the east and was not considered further due to lack of corroborating data. The 111 samples collected represented 47% of the total precipitation during the sampling period (Table 1).

Table 1. Annual total precipitation (tPrecip, mm) and in the events sampled by Fritz et al. (2021; rPrecip, mm). Percent indicates the proportion of precipitation represented in the samples collected by Fritz et al. (2021).

	n	rPrecip	tPrecip	Percent
Aug – Dec 2015	21	71.7	168.9	43%
Jan – Dec 2016	34	100.2	203.5	49%
Jan – Dec 2017	26	113.4	278.3	41%
Jan – Aug 2018	30	113.8	200.8	57%
Total	111	399.3	851.5	47%

3.4 Precipitation 1985–1995

Precipitation at Inuvik Airport, 12 km southeast of Inuvik, was collected monthly from December 1985 to March 1986 and December 1987 to May 1995, by the Atmospheric Environment Service, Environment Canada.

The precipitation received at the rain or snow gauge was stored daily in a sealed Nalgene bottle, with all precipitation collected in a calendar month blended. At the end of each month, samples were decanted into vials, sealed and sent for stable isotope analysis at the University of Waterloo Isotope Laboratory (December 1985 to February 1989) or the University of Western Ontario Department of Geology (March 1989 to May 1995).

The data processed by the University of Waterloo were released by the laboratory to the Global Network of Isotopes in Precipitation (GNIP) and were available to Fritz et al. (2022) for comparative analysis of co-isotope ratios in precipitation at Inuvik in 1985–1989. The data generated at the University of Western Ontario are presented in the Appendix at the end of this paper.

4 RESULTS

Table 2 presents the distribution of precipitation events by origin. The distribution of samples collected by Fritz et al. (2022) is representative of the broader population at Inuvik during the sampling period. The proportions of sampled events were 66, 21, and 12% from the north, west, and south, respectively, and for all events with ≥ 0.1 mm of precipitation the proportions were 60, 26, and 13%. The remaining 1% came from the east.

Table 2. Mean values of $\delta^{18}O$ (‰) and temperature (T, °C) for sampled storms, stratified by season and direction of origin. Data for $\delta^{18}O$ from Fritz et al. (2021). Total n represents the total number of storms during the sampling period in 2015–2018. Also included is the standard error of the mean (SE) for both $\delta^{18}O$ and T.

	Sample n	Total n	$\delta^{18}O$	T	$\delta^{18}O$ (SE)	T (SE)
North	74	264	-19	-1.1	0.6	1.5
Winter	20	137	-24.3	-17.6	0.7	1.0
Summer	54	127	-16.7	5.8	0.5	0.9
South	14	115	-21	0.9	1.3	2.5
Winter	6	84	-25.2	-7.1	1.0	2.2
Summer	8	31	-17.8	6.8	1.2	2.6
West	23	59	-20.5	-1.4	0.8	3.0
Winter	11	36	-23.3	-14.4	1.0	2.5
Summer	12	23	-18	10.4	0.8	1.5
Total	111	438	-19.6	-1	0.5	1.2
Winter	37	257	-25.1	-15.9	0.6	1.4
Summer	74	181	-17.5	6.7	0.3	0.6

4.1 Storm Origin and Stable Isotope Concentration

The data presented by Fritz et al. (2021) were sorted by their origin from the north, south, east, or west depending on the HYSPLIT analyses for each event. Precipitation from the north originated in the Arctic Ocean, from the south in the Pacific Ocean, and from the west in the Bering Sea, Sea of Okhotsk, or Chukchi Sea. The data were further classified as winter (October–April) or summer (May–September) events.

Overall, the $\delta^{18}O$ values in precipitation show only small differences in mean $\delta^{18}O$ when the samples are separated by direction of origin and grouped for both or either season (Table 2). Figure 2a presents box-and-whisker plots of the $\delta^{18}O$ values grouped by direction of origin that show similarity in distribution between the three groups in each season. Student's t-tests for differences between these various groups (north, south, west) by season (all year, summer, winter) did not show any statistically significant (α = 0.05) differences between the mean values of the seasonal groups.

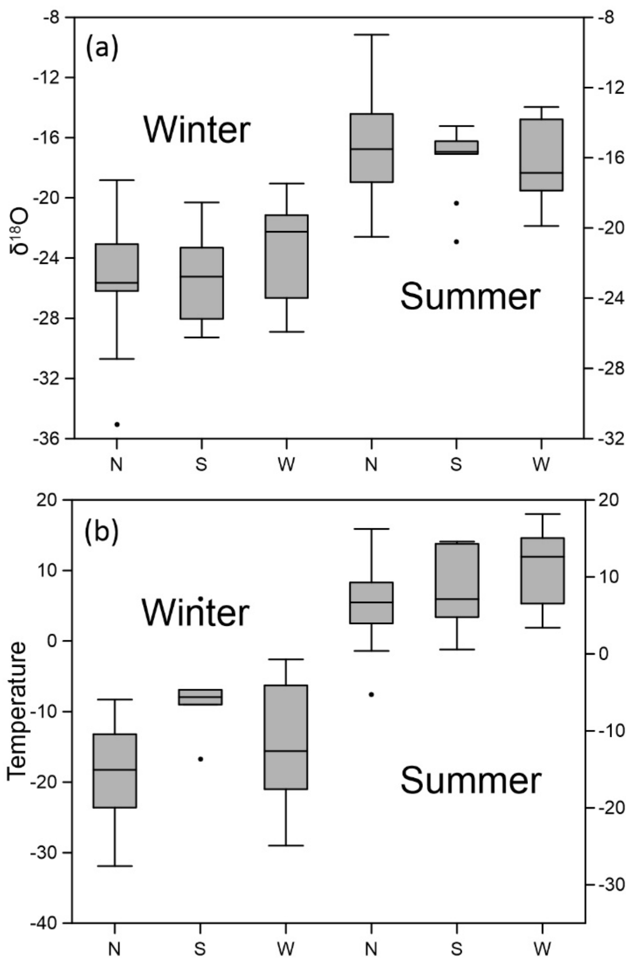

Figure 2. (a) Box-and-whisker plots of $\delta^{18}O$ (‰) grouped by direction of origin and season. (b) Mean temperature (°C) on day of precipitation grouped by origin and season.

4.2 Atmospheric Temperature and Stable Isotopic Concentration

4.2.1 Event by Event

Most precipitation events (66%) originated from the north and were associated with the lowest mean daily temperatures in summer and winter but not the lowest $\delta^{18}O$ values. In fact, during the summer months, storms from the north had the highest $\delta^{18}O$ values.

Precipitation originating in the south represented 12% of the sampled events and had relatively low $\delta^{18}O$ values. In the winter, storms from the south had $\delta^{18}O$ values 1‰ lower than northern storms but, on average, were associated with mean daily temperatures about 10 °C higher.

Western storms had the highest $\delta^{18}O$ values in winter, but the lowest in summer, despite coinciding with the warmest mean summer conditions. Overall, the results do not conform to equation 3, because the highest temperatures in summer and winter are associated with the lowest values of precipitation $\delta^{18}O$ in these seasons.

Box-and-whisker plots for mean temperature during precipitation events show considerable overlap in the distribution associated with the three directions of origin in summer but not in winter (Figure 2b). A series of t-tests indicated a statistically significant ($\alpha = 0.05$) difference in mean temperature between winter events from the north and south, and from the south and west. Similarly, in the summer there was a statistically significant difference in mean temperature between storms from the north and west, and from the south and west. The significant difference in temperature between groups without significant difference in $\delta^{18}O$ suggests that the $\delta^{18}O$:T relations for each group may not be the same.

The least-squares linear regression line fitted to the whole data set has a statistically significant slope and a coefficient of determination (R^2) of 0.59; the regression lines for the events from the north, south, and west over the year have similar R^2 (Table 3). The regression coefficients vary for the different origins but are not statistically different at $\alpha = 0.05$. The intercepts are all close to the mean values for $\delta^{18}O$ because mean T is close to 0 °C (Table 2). Figure 3 is a plot of $\delta^{18}O$ values and temperature for all sampled precipitation events. Visually, it is evident that the data plot into two groups representing summer and winter precipitation events.

Table 3. Least-squares linear regression lines for $\delta^{18}O$ on temperature from all samples collected in 2015–2018 and sorted by direction and season. Data for $\delta^{18}O$ from Fritz et al. (2021).

Origin	n	equation	R^2	p
North	74	0.33T – 18.7	0.64	<0.001
South	14	0.40T – 21.3	0.62	<0.001
West	23	0.22T – 20.2	0.60	<0.001
All Directions	111	0.30T – 19.3	0.59	<0.001
Summer	74	0.19T – 18.2	0.01	0.007
Winter	37	0.16T – 22.2	0.15	0.02

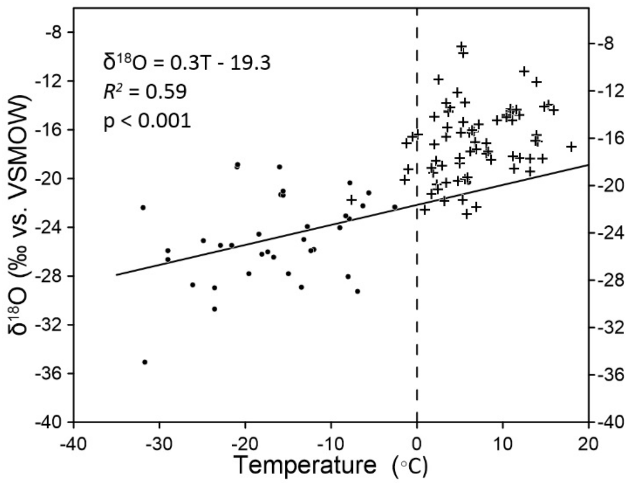

Figure 3. Scatterplot of temperature and $\delta^{18}O$ for summer (+) and winter storms (•) at Inuvik in 2015–2018 with least-squares linear regression line fitted to all data.

4.2.2 Seasonal Precipitation

In summer, the isotopic composition of rain from northern and western storms had significant relations with temperature at $\alpha = 0.05$ (Table 4). None of the relations from winter data for specific directions were statistically significant (Table 4). Figure 4 plots data from the summer and winter seasons collected from 2015–2018. The regression coefficients for both seasons are statistically significant at $\alpha = 0.05$, but both present low R^2 (Table 3), indicating little of the variation in $\delta^{18}O$ is explained by variation in T.

4.2.3 Monthly Aggregate Sampling

The least-squares linear regression lines for $\delta^{18}O$:T using all data from 1985–1995 present regression coefficients similar to the relation for 2015–2018 (Tables 3 and 5). The similarity of slope and intercept suggest that the relations between $\delta^{18}O$ and temperature are consistent at the time scales of individuals events and on a monthly basis (Tables 3 and 5). The higher coefficients of determination for the seasonal relations between $\delta^{18}O$ and temperature (Table 5) may be associated with signal smoothing for the differing

Table 4. Least-squares linear regression lines for $\delta^{18}O$ on temperature from summer and winter samples taken in 2015–2018 separated by direction. Data for $\delta^{18}O$ from Fritz et al. (2021).

Origin	n	equation	R^2	p
Summer				
North	54	0.24T – 18.1	0.13	0.01
South	8	0.11T – 18.5	0.05	0.58
West	12	0.35T – 21.6	0.47	0.01
Winter				
North	20	0.22T – 21.2	0.15	0.09
South	6	0.28T – 23.3	0.37	0.2
West	11	0.16T – 21.0	0.16	0.22

time unites of sample collection. The δ18O and temperature values for 1985–1995 are monthly means. In summer, precipitation generally occurs on cool days but in winter relatively cold days are characteristically dry.

4.3 Physiographic Influences on Stable Isotopic Concentration

Table 6 presents data on the characteristics of precipitation arriving at Inuvik directly from the Beaufort Sea and in atmospheric systems that have crossed mountain ranges. Year-round, systems that passed over mountains resulted in δ18O values 1‰ lower than those that did not (Table 6). However, t-tests for these data sorted by season indicated no statistically significant ($\alpha = 0.05$) difference between mean δ18O for storms that travelled over mountains and those that did not. In contrast, t-tests for mean temperature on the day of the storm show a statistically significant difference during the summer between storms that passed over mountains and those that arrived directly from the Arctic Ocean.

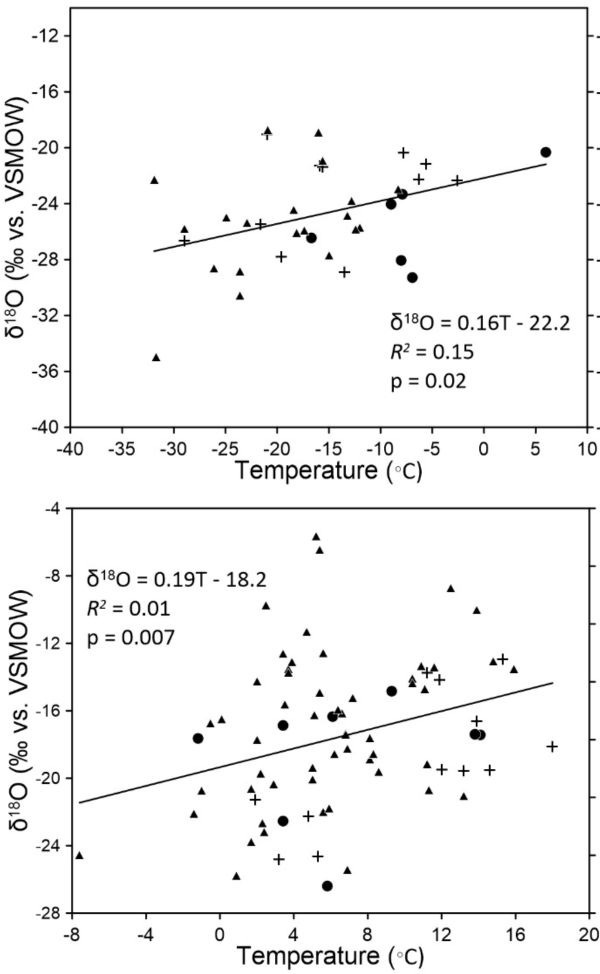

Figure 4. Scatterplots of temperature and δ18O for (a) summer and (b) winter events from 2015–2018, with northern (▲), southern (•), and western (+) origins. The line has been fitted by least-squares linear regression.

Table 5. Least-squares linear regression for δ18O on temperature from all monthly aggregate samples collected from 1985–95 and separated by season. Data for δ18O and temperature are in the Appendix.

	n	equation	R^2	p
All data	91	0.31T – 21.9	0.71	<0.001
Summer	34	0.46T – 23.0	0.55	<0.001
Winter	57	0.26T – 23.0	0.28	<0.001

Table 6. Mean values of δ18O (‰) and temperature (T, °C) of storms that passed over mountains (Yes) and those that did not (No). Also included is the standard error of the mean (SE) for both δ18O and T.

Mountain Transit	n	δ18O	T	δ18O (SE)	T (SE)
Winter					
Yes	16	-25.4	-14.1	0.7	1.5
No	21	-24.1	-17.4	1.1	2.5
Summer					
Yes	19	-17.5	9.3	0.4	0.7
No	55	-16.5	5.7	0.6	0.9

The orographic influence on isotope composition in precipitation is illustrated in Figure 5. Figure 5a displays the tracks of two storms with precipitation that fell at -32 °C. One, on 23 January 2017, had an δ18O value of -35.1‰. It originated over the Arctic Ocean but travelled over the Brooks Range and Yukon mountains before arriving at Inuvik. The other, arriving directly from the Arctic Ocean 17 days later on 10 February 2017, brought precipitation with an δ18O value of -22.4‰. The contrast in δ18O between the storms is likely due to fractionation during condensation within the first air mass as it passed over several mountain ranges.

A similar example is presented from autumn 2015 in Figure 5b, which illustrates the path of a southerly storm and a northerly storm. The storm from the south passed over several mountain ranges and had precipitation at Inuvik with a lower δ18O value than the northern storm, even though it arrived under warmer conditions. These examples represent the overall statistics presented in Table 2 regarding storms from the North and South.

5 Discussion

5.1 Physiographic Effects

Figure 5 and Table 6 show that orographic features influence the isotopic composition of air masses delivering precipitation to Inuvik. The absolute difference in δ18O value between precipitation from air masses derived from the Arctic Ocean directly and those that travelled over mountains is not statistically significant at $\alpha = 0.05$, but there is a statistically significant difference in summer mean temperatures between these precipitation events (Table 6). In North America, δ18O in precipitation decreases by 0.28‰ for every increase of 100 m in elevation (Poage and Chamberlain 2001), a relation that is constant throughout

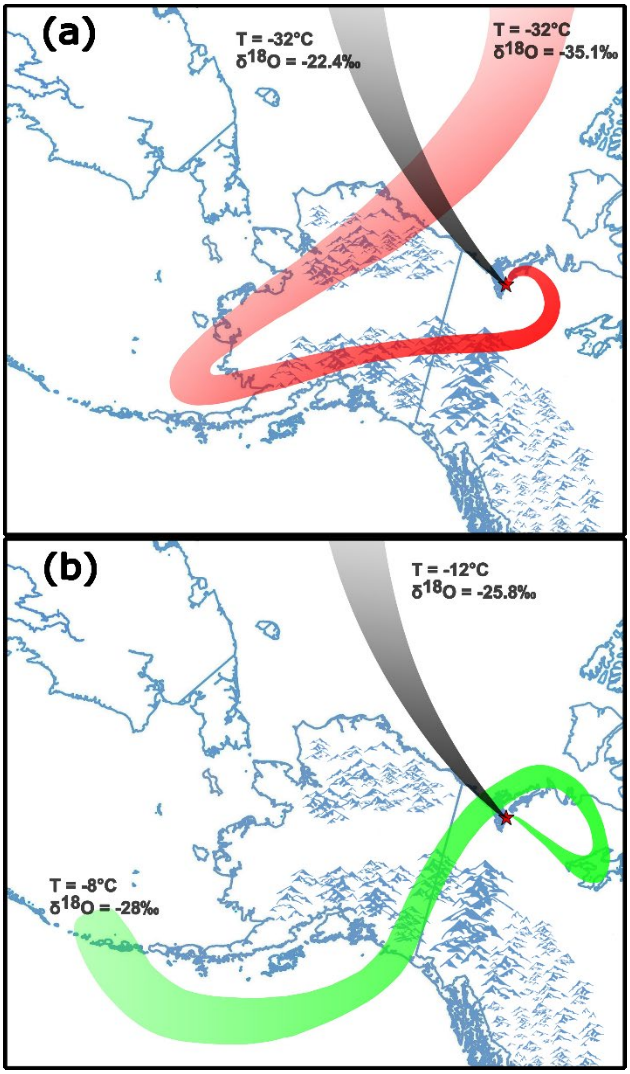

Figure 5. Illustration of storm trajectories derived from the HYSPLIT model. All trajectories show 13 days of travel. Red trajectory in (a) represents the path taken by the air mass responsible for an event on 23 January 2017; the black trajectory represents a path up to 10 February 2017. The black trajectory in (b) represents the path taken by the air mass responsible for an event on 29 October 2015; the green trajectory represents a path up to 2 November 2015.

the world, except at very high altitude (> 5000 m a.s.l) and in the Himalayas. When applied to the Canadian western Arctic, the influence of fractionation during southerly passage over mountains lowers $\delta^{18}O$ to values similar to those derived from the cold source in the Arctic Ocean nearby.

Westerly and southerly storms have $\delta^{18}O$ values similar to northern storms despite being associated with warmer air temperatures. Air masses from the south and west pass over the Coast and St. Elias mountains upon landfall, and Mackenzie Mountains once farther inland (Figure 1). Western storms typically pass over the Brooks Range in Alaska and Richardson Mountains before reaching Inuvik (Figure 1). Occasionally, air masses from the west made landfall over eastern Siberia, travelling over the Chukotka Mountains.

5.2 $\delta^{18}O$:T Relations

The regression coefficients reported here are lower than for precipitation in Antarctica (0.57‰ °C^{-1}) and Siberia (0.50‰ °C^{-1}; Schlosser et al. 2004; Kostrova et al. 2020). The coefficients for all storms (e.g., 0.3‰ °C^{-1}; Tables 3 and 4) are lower than the slope determined by Porter et al. (2016) for mid-high-latitude North America (0.41‰ °C^{-1}). Porter et al. (2016) demonstrate that the western Canadian Arctic has a relatively low slope for $\delta^{18}O$:T. The even lower slopes derived when storms from 2015–2018 were separated by season and direction illustrates the complexity of these relations in the specific physiographic location of Inuvik (Table 4).

At a monthly timescale, as summarized in Table 5, the coefficients are similarly lower than data from Antarctica and Siberia, but in winter, especially, the coefficient of determination indicates a weak relation.

5.3 Influence on Ground Ice

Mackay (1983a) indicated characteristic values for $\delta^{18}O$ in various types of ground ice in western Arctic Canada. He gave a range of -18 to -20‰ for the $\delta^{18}O$ value in active layer ice. Summer precipitation from 1985–1995 had $\delta^{18}O$ values consistent with this range (see Appendix). More recently, higher $\delta^{18}O$ values have been observed (Table 2). He associated aggradational ice, i.e., the transient layer, with active layer ice now incorporated in permafrost (Mackay 1983b). He associated wedge ice (-22 to -26‰) with winter precipitation (Mackay, 1990). The $\delta^{18}O$ values for precipitation collected from 1985–1995 are below this range (see Appendix). However, they are consistent with the recent winter precipitation (Table 2). The origin of wedge ice from snow melt implies that its $\delta^{18}O$ values should be consistent with winter precipitation. In this case, the precipitation at the time of Mackay's sampling probably had lower $\delta^{18}O$ values than recently, as suggested by the 1985–95 data. Michel (1990) also noted inconsistencies between $\delta^{18}O$ in ice wedges and regional winter precipitation. Such uncertainty reduces confidence in granular interpretation of paleoclimate from wedge ice sequences over and above the weakness of the isotope-climate relations from analysis of individual storms presented here.

6 Conclusions

We draw four principal conclusions:

(1) In the western Canadian Arctic, the isotopic composition of precipitation from different source areas is relatively consistent during the summer and winter seasons because fractionation during transport over mountains to the south or west induces a similar stable isotopic composition as in precipitation coming from the Arctic Ocean.

(2) $\delta^{18}O$:T relations in precipitation at Inuvik vary with the origin of air masses and by season. The regression coefficients for $\delta^{18}O$ on T of data collected from individual

storms in summer 2015–2018 ranged from 0.11 to 0.35‰ °C^{-1} and from 0.16 to 0.28‰ °C^{-1} in winter.

(3) R^2 for $\delta^{18}O$ on T for individual events by season in 2015–2018 were ≤ 0.47 in summer and ≤ 0.37 in winter. None of the winter relations between $\delta^{18}O$ and T were statistically significant at α = 0.05. The relations derived from aggregate samples had R^2 ≤ 0.55 in summer and winter and were statistically significant.

(4) Aggregate $\delta^{18}O$:T relations for precipitation and temperature at Inuvik, derived from all precipitation and using monthly mean temperature, deliver regression coefficients of 0.46 and 0.26‰ °C^{-1} in summer and winter, respectively.

Overall, these results indicate the relations between $\delta^{18}O$ and T at a near-coastal location in western Arctic Canada are weak when derived on an event-by-event basis but are statistically stronger from smoothed aggregate samples.

7 Acknowledgements

We thank Trevor Andersen for assistance with the HYSPLIT model and with the climate record for Inuvik. Ian McKendry drew our attention to HYSPLIT. Isotopic data generated at the University of Western Ontario were kindly provided by Professor Fred Longstaffe. The research was supported by an NSERC Discovery Grant. Our field research in the western Arctic was also supported by the Aurora Research Institute and the Polar Continental Shelf Project of Natural Resources Canada. We would also like to thank Alberto Reyes and an anonymous reviewer for their valuable comments on this paper.

8 References

Burn, C.R., Michel, F.A., and Smith, M.W. 1986. 'Stratigraphic, Isotopic and Mineralogical Evidence for an Early Holocene Thaw Unconformity at Mayo, Yukon Territory', *Canadian Journal of Earth Sciences* 23(6), pp. 794–803. doi:10.1139/e86-081.

Chylek, P., Folland, C., Klett, J.D., Wang, M., Hengartner, N., Lesins, G., and Dubey, M.K. 2022. 'Annual Mean Arctic Amplification 1970–2020: Observed and Simulated by CMIP6 Climate Models', *Geophysical Research Letters* 49(13). doi:10.1029/2022gl099371.

Craig, H. 1961. 'Isotopic Variations in Meteoric Waters', *Science* 133(3465), pp. 1702–1703.

Dansgaard, W. 1964. 'Stable Isotopes in Precipitation', *Tellus* 16(4), pp. 436–468. doi:10.1111/j.2153-3490.1964.tb00181.x.

Environment Canada 2023. *Historical Climate Data, Inuvik Airport (2015–2018)*. Available at: https://climate.weather.gc.ca/index_e.html.

Fritz, M., Wetterich, S., McAlister, J., and Meyer, H. 2021. 'Stable Oxygen (δ18O) and Hydrogen (δD) Isotopes in Precipitation from Inuvik in the Western Canadian Arctic (2015–2018)', *PANGAEA* [dataset], https://doi.org/10.1594/PANGAEA.935027.

Fritz, M., Wetterich, S., McAlister, J., and Meyer, H. 2022. 'A New Local Meteoric Water Line for Inuvik (NT, Canada)', *Earth System Science Data* 14(1), pp. 57–63. doi:10.5194/essd-14-57-2022.

Gonfiantini, R. 1978. 'Standards for Stable Isotope Measurements in Natural Compounds', *Nature* 271(5645), pp. 534–536. doi:10.1038/271534a0.

Holland, K.M., Porter, T.J., Froese, D.G., Kokelj, S.V. and Buchanan, C.A. 2020. 'Ice-Wedge Evidence of Holocene Winter Warming in the Canadian Arctic', *Geophysical Research Letters* 47(12). doi:10.1029/2020GL087942.

Kostrova, S.S., Meyer, H., Fernandoy, F., Werner, M., and Tarasov, P.E. 2020. 'Moisture Origin and Stable Isotope Characteristics of Precipitation in Southeast Siberia', *Hydrological Processes* 34(1), pp. 51–67. doi:10.1002/hyp.13571.

Kotler, E. and Burn, C.R. 2000. 'Cryostratigraphy of the Klondike "Muck" Deposits, West-Central Yukon Territory', *Canadian Journal of Earth Sciences* 37(6), pp. 849–861. doi:10.1139/e00-013.

Mackay, J.R. 1983a. 'Oxygen Isotope Variations in Permafrost, Tuktoyaktuk Peninsula Area, Northwest Territories', *Geological Survey of Canada* Paper 83-1B, pp. 67–74. doi:10.4095/132539.

Mackay, J.R. 1983b. 'Downward Water Movement into Frozen Ground, Western Arctic Coast', *Canadian Journal of Earth Sciences* 20(1), pp. 120–134. doi:10.1139/e83-012.

Mackay, J.R. 1990. 'Some Observations on the Growth and Deformation of Epigenetic, Syngenetic and Anti-Syngenetic Ice Wedges', *Permafrost and Periglacial Processes* 1(1), pp. 15–29. doi:10.1002/ppp.3430010104.

Michel, F.A. 1990. 'Isotopic Composition of Ice-Wedge Ice in Northwestern Canada', in *5th Canadian Permafrost Conference*. Québec City, Québec, Canada: June 6–8, 1990, pp. 5–9.

Meyer, H., Opel, T., Laepple, T., Dereviagin, A.Y., Hoffmann, K., and Werner, M. 2015. 'Long-Term Winter Warming Trend in the Siberian Arctic During the Mid- to Late Holocene', *Nature Geoscience* 8(2), pp. 122–125. doi:10.1038/ngeo2349.

Opel, T., Laepple, T., Meyer, H., Dereviagin, A.Y., and Wetterich, S. 2017. 'Northeast Siberian Ice Wedges Confirm Arctic Winter Warming Over the Past Two Millennia', *The Holocene* 27(11), pp. 1789–1796. doi:10.1177/0959683617702229.

Poage, M.A. and Chamberlain, C.P. 2001. 'Empirical Relationships Between Elevation and the Stable Isotope Composition of Precipitation and Surface Waters: Consideration for Studies of Paleoelevation Change', *American Journal of Science* 301(1), pp. 1–15. doi:10.2475/ajs.301.1.1.

Porter, T.J., Froese, D.G., Feakins, S.J., Bindeman, I.N., Mahony, M.E., Pautler, B.G., Reichart, G.J., Sanborn, P.T., Simpson, M.J., and Weijers, J.W.H. 2016. 'Multiple Water Isotope Proxy Reconstruction of Extremely Low Last Glacial Temperatures in Eastern Beringia (Western Arctic)', *Quaternary Science Reviews*, pp. 113–125. doi:10.1016/j.quascirev.2016.02.006.

Schetselaar, A., Andersen, T., and Burn, C.R. 2023. 'Performance of Climate Projections for Yukon and Adjacent Northwest Territories, 1991–2020', *Arctic* 76(3), pp. 244–264. doi:10.14430/arctic77263.

Schlosser, E., Reijmer, C., Oerter, H., and Graf, W. 2004. 'The Influence of Precipitation Origin on the δ^{18}O:T Relationship at Neumayer Station, Ekstrmisen, Antarctica', *Annals of Glaciology*, pp. 41–48. doi:10.3189/172756404781814276.

Serreze, M.C. and Barry, R.G. 2011. 'Processes and Impacts of Arctic Amplification: A Research Synthesis', *Global and Planetary Change* 77(1), pp. 85–96. doi:10.1016/j.gloplacha.2011.03.004.

Stein, A.F., Draxler, R.R., Rolph, G.D., Stunder, B.J.B., Cohen, M.D., and Ngan, F. 2015. 'NOAA's HYSPLIT Atmospheric Transport and Dispersion Modeling System', *Bulletin of the American Meteorological Society* 96(12), pp. 2059–2077. doi:10.1175/BAMS-D-14-00110.1.

Thienpont, J.R., Rühland, K.M., Pisaric, M.F.J., Kokelj, S.V., Kimpe, L.E., Blais, J.M., and Smol, J.P. 2013. 'Biological Responses to Permafrost Thaw Slumping in Canadian Arctic Lakes', *Freshwater Biology* 58(2), pp. 337–353. doi: 10.1111/fwb.12061.

Appendix. Mean monthly temperature (T, °C), total monthly precipitation (P, mm), and δ^{18}O (‰) for aggregate samples of monthly precipitation collected at Inuvik Airport between March 1989 and May 1995.

Date	T	P	δ^{18}O	Date	T	P	δ^{18}O	Date	T	P	δ^{18}O
03/1989	-23.5	4.4	-25.0	**04/1991**	-8.2	6.0	-23.1	**06/1993**	12.6	3.7	-11.4
04/1989	-9.4	1.6	-28.7	**05/1991**	5.9	20.6	-18.3	**07/1993**	15.2	29.2	n/a
05/1989	0.5	18.7	-23.7	**06/1991**	10.5	33.4	-18.2	**08/1993**	11.0	41.6	-20.8
06/1989	12.3	20.2	-14.8	**07/1991**	12.4	16.7	-16.6	**09/1993**	4.2	30.6	-18.2
07/1989	16.5	63.2	-16.8	**08/1991**	9.1	73.2	-20.2	**10/1993**	-4.3	27.3	-24.4
08/1989	15.5	32.8	-16.9	**09/1991**	4.2	41.5	-19.3	**11/1993**	-17.8	13.9	-26.8
09/1989	5.3	53.9	-19.0	**10/1991**	-7.5	29.6	-23.4	**12/1993**	-23.1	19.6	-27.4
10/1989	-8.2	36.8	-28.3	**11/1991**	-24.1	13.1	-32.5	**01/1994**	-31.1	4.0	n/a
11/1989	-27.9	11.0	-34.4	**12/1991**	-29.2	9.3	-25.6	**02/1994**	-27.3	21.2	-28.9
12/1989	-26.1	11.4	-27.6	**01/1992**	-28.7	24.0	-29.8	**03/1994**	-21.9	26.1	-30.6
01/1990	-32.7	18.4	-30.5	**02/1992**	-28.2	14.8	-23.3	**04/1994**	-12.3	14.8	-16.9
02/1990	-34.3	9.0	-31.2	**03/1992**	-16.2	11.4	-24.5	**05/1994**	3.0	20.0	-20.8
03/1990	-16.3	19.6	-30.8	**04/1992**	-15.3	28.1	-27.5	**06/1994**	10.3	31.9	-18.2
04/1990	-7.7	13.1	-24.6	**06/1992**	11.8	17.1	-19.2	**07/1994**	18.3	26.0	-14.4
05/1990	1.6	0.2	n/a	**07/1992**	14.2	26.6	-17.8	**08/1994**	14.9	44.5	-15.5
06/1990	11.3	16.0	-21.9	**08/1992**	11.7	29.0	-18.3	**09/1994**	1.2	31.7	-21.4
07/1990	15.5	58.0	-18.8	**09/1992**	-1.4	48.2	-24.9	**10/1994**	-5.3	21.4	-23.9
08/1990	9.7	10.2	-15.1	**10/1992**	-10.6	26.8	-21.5	**11/1994**	-22.8	34.7	-32.5
09/1990	3.2	31.7	-21.9	**11/1992**	-19.0	14.8	-28.2	**12/1994**	-25.2	19.7	-34.1
10/1990	-7.4	25.8	-29.3	**12/1992**	-24.7	19.1	-28.7	**01/1995**	-23.6	8.0	-29.4
11/1990	-26.9	20.8	-26.7	**01/1993**	-22.8	27.5	-29.5	**02/1995**	-26.0	23.2	-29.1
12/1990	-28.7	12.4	-28.4	**02/1993**	-21.3	23.2	-27.5	**03/1995**	-25.0	23.2	-28.4
01/1991	-25.0	20.0	-28.3	**03/1993**	-18.8	6.6	-26.0	**04/1995**	-7.5	3.3	-17.1
02/1991	-28.5	13.4	-33.4	**04/1993**	-1.5	5.6	-22.5	**05/1995**	5.3	25.6	-22.9
03/1991	-23.6	19.2	-29.2	**05/1993**	0.9	8.6	-28.1				
Winter (October–April) Mean δ^{18}O 1985–1995:						**-28.2**					
Summer (May–September) Mean δ^{18}O 1985–1995:						**-19.2**					
Annual Mean δ^{18}O 1985–1995:						**-24.8**					
Winter (October–April) Mean δ^{18}O 1989–1995:						**-27.5**					
Summer (May–September) Mean δ^{18}O 1989–1995:						**-19.5**					
Annual Mean δ^{18}O 1989–1995:						**-24.3**					